

Model of vitreous SiO₂ generated by an *ab initio* molecular-dynamics quench from the melt

Johannes Sarnthein

*Institut Romand de Recherche Numérique en Physique des Matériaux (IRRMA), IN-Ecublens,
CH-1015 Lausanne, Switzerland,
and Institut für technische Elektrochemie, Technische Universität Wien, A-1060 Wien, Austria*

Alfredo Pasquarello

*Institut Romand de Recherche Numérique en Physique des Matériaux (IRRMA), IN-Ecublens,
CH-1015 Lausanne, Switzerland*

Roberto Car

*Institut Romand de Recherche Numérique en Physique des Matériaux (IRRMA), IN-Ecublens,
CH-1015 Lausanne, Switzerland,
and Département de la Matière Condensée, Université de Genève, CH-1211 Genève, Switzerland*

(Received 5 May 1995; revised manuscript received 22 June 1995)

We studied liquid and vitreous SiO₂ by performing first-principles molecular-dynamics simulations. Diffusion in the liquid is shown to occur through correlated jump events, which disrupt the network only for short time periods. The persistence of the network even at high temperatures is confirmed by the average structural properties of the liquid. By quenching from the melt, we obtained a model for the glass, which forms a perfectly chemically ordered network. Structural and electronic properties of our model glass present a remarkable agreement with vitreous SiO₂: the calculated total structure factor closely agrees with data from neutron diffraction experiments and features in the *x*-ray photoemission spectrum are well reproduced by the electronic density of states. This agreement strongly supports other structural properties which are yet unavailable from experiment such as partial pair correlation functions and bond-angle distributions. A comparative study of the electronic density of states in liquid, vitreous, and crystalline SiO₂ shows that enhancement of disorder gives rise to a reduction of the gap.

I. INTRODUCTION

Besides their fundamental importance as network forming systems and as principal constituents of the earth mantle, disordered forms of silicon dioxide (SiO₂) play a key role in the glass manufacturing industry as well as in electronic device applications.¹⁻⁴

During the last two decades, molecular-dynamics (MD) studies have significantly contributed to the understanding of the structural properties of disordered forms of SiO₂.⁵⁻⁸ In these simulations, the interaction between atoms is described by empirical classical potentials.

The remarkable characteristic of SiO₂ to exist in a multitude of allotropic forms⁹ is related to the peculiar mixture of ionic and covalent contributions to the Si-O bond. Hence an explicit treatment of the electronic structure, sensitive to the particular structural environment, is expected to give a definite improvement to the description of disordered forms of SiO₂. In addition, such a description would provide access to the electronic properties of these systems, which are missed by classical studies.

First-principles approaches provide an appropriate tool for such studies. Indeed, these methods have already been successfully applied to the study of crystalline SiO₂.¹⁰⁻¹² However, their application to disordered forms of SiO₂ has so far been precluded by several difficulties. The complexity of these systems consists in the necessity of studying a large

number of atoms. Moreover, a major obstacle has been the presence of oxygen atoms, which require prohibitively large basis sets when treated with plane waves and conventional pseudopotentials (PP's).

We have performed *ab initio* molecular-dynamics simulations of liquid and vitreous SiO₂, using the Car-Parrinello (CP) method^{13,14} in conjunction with Vanderbilt's ultrasoft PP's.¹⁵ The augmentation scheme of these PP's allowed us to treat rather localized electronic states, such as those that occur in the presence of oxygen atoms, with a substantially smaller number of plane waves compared to the case of conventional PP's. In this way, much larger systems became affordable and the study of disordered forms of SiO₂ was made possible.

We started our investigation by studying the diffusion in the liquid. Liquid SiO₂ is characterized by the presence of a strong underlying network which is only occasionally disrupted to allow diffusion. In order to obtain a model for vitreous SiO₂, we quenched the system to 300 K. The resulting structure was perfectly chemically ordered, i.e., every silicon and every oxygen atom was fourfold and twofold coordinated, respectively.

In a previous paper, we have reported on some aspects of these simulations.¹⁶ For the amorphous, a comparison of calculated and experimental neutron structure factors showed excellent agreement. Partial structure factors provided a basis to characterize the first sharp diffraction peak (FSDP), which

has recently been a subject of debate.^{8,17–20} We found that the Si-Si, Si-O, and O-O partial structure factors all contribute to the FSDP, and that this peak does not arise from a peak in the concentration-concentration structure factor $S_{CC}(q)$.^{21,19} The calculated electronic density of states reproduced well features observed by x-ray photoemission; in particular, differences between the spectra of vitreous and α -crystalline SiO₂ were accounted for. Furthermore, an analysis of the localization properties of the wave functions suggested a qualitative explanation for the different mobilities of electrons and holes in vitreous SiO₂.

In this work, we present complementary information extracted from the same simulations. In particular, we focus on aspects of the diffusion mechanism in the liquid, on a more extended analysis of the structural properties of the liquid and of the amorphous, and on the dependence of the electronic density of states on disorder and temperature. We show that diffusion events in the liquid consist of temporary defects created by sudden neighbor exchanges, which are subsequently immediately restored. The structural properties are analyzed through the partial pair correlation functions and the bond-angle distributions. Finally, we have studied as a function of temperature the dependence of the electronic gap in liquid, vitreous, and α -crystalline SiO₂.

The paper is organized as follows. In Sec. II, we briefly describe the method and give technical details of the simulation. Some aspects of the diffusion in liquid SiO₂ are presented in Sec. III. Structural properties and electronic properties are the subject of Secs. IV and V, respectively. The paper concludes with Sec. VI.

II. MOLECULAR-DYNAMICS SIMULATION: TECHNICAL ASPECTS

We performed constant volume CP molecular dynamics,^{13,14} in which the electronic structure was treated within the local density approximation (LDA) to density functional theory. Most of the technical aspects of the simulation have been given in Ref. 16 and a detailed description of our approach can be found in Ref. 22. We give here only a brief summary of the conditions of the simulations and refer to the above references for more details.

In our simulation of liquid SiO₂ we used a periodically repeated cubic cell of side 10.45 Å containing $\mathcal{N}=72$ atoms. This corresponds to a density of 2.10 g/cm³. We started our MD simulation from a configuration of the liquid as generated by Monte Carlo using an empirical potential.⁸

The system was allowed to evolve at temperatures ranging from 2500 to 3500 K for more than 6 ps. Then the temperature was fixed at 3500 K, well above the experimental melting point of $T_m=2000$ K, since only at such a high temperature was diffusion in our system sufficiently fast to produce an equilibrated liquid in the time span of the simulation. After 3 ps of equilibration, the actual measurements were taken in the following 5 ps. Then we set the temperature of our system to 3000 K and took measurements for 3 ps to investigate the effects of cooling. The diffusion that took place during the simulation at 3000 K was already almost negligible. Finally we quenched the system to 300 K in another 3 ps, obtaining a model for vitreous SiO₂.

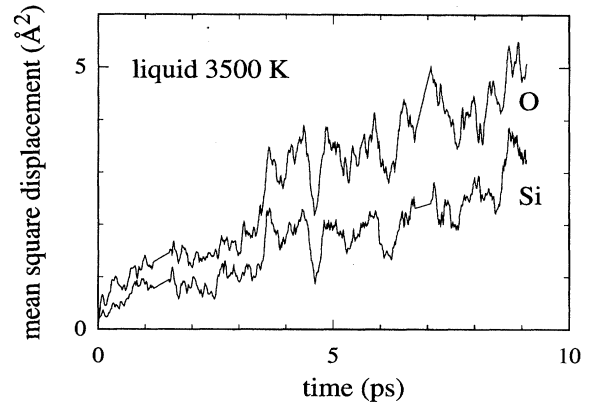


FIG. 1. Mean square displacement of Si and O in liquid SiO₂ at 3500 K.

III. DIFFUSION IN LIQUID SiO₂

The mean square displacement corresponding to the simulation of the liquid at 3500 K shows diffusive motion, as can be seen in Fig. 1. From our simulation, we estimate diffusion constants $D_{\text{Si}}=(5\pm 1)\times 10^{-6}$ cm²/s for silicon and $D_{\text{O}}=(9\pm 2)\times 10^{-6}$ cm²/s for oxygen.²³ The ratio of these two constants can be explained in terms of the mass ratio of the two elements. A strong correlation between oxygen and silicon motions can be noticed in Fig. 1. This feature can be associated to the persistence of a network even at these high temperatures (see Sec. IV A.).

Various pieces of evidence point towards the fact that the simulated liquid is equilibrated. We found that on average each Si atom has moved by more than 2 Å and each O atom by more than 2.7 Å from the initial configuration obtained with the classical Hamiltonian. Given the diffusive motion in Fig. 1 and that the typical value for the Si-O bond length is 1.6 Å, these are sufficiently large diffusion lengths for the system to reach equilibration. This is confirmed by monitoring during the simulation the average structural properties such as the partial pair correlation functions and the bond-angle distributions. After an initial transient of a few ps in which a noticeable change led to substantially broader distributions of bond lengths and angles compared to the initial configuration, no subsequent drift was observed.

In order to get insight in the diffusion mechanisms in liquid SiO₂, we have studied relative distances between silicon and nearest-neighbor oxygen atoms. To illustrate a typical diffusive event, we have reported in Fig. 2 the radial distances of nearest-neighbor oxygen atoms from a given silicon atom as a function of time. The trajectories of the nearest oxygen atoms have been labeled. At the beginning of the period shown in Fig. 2 the considered silicon atom was fourfold coordinated, with all other oxygen atoms being at least as far as 2.5 Å. Suddenly, in a time span of less than ≈ 0.1 ps, one oxygen atom (labeled No. 4) diffused away, leaving the Si atom threefold coordinated. A complex pattern of trajectories followed during 0.2 ps with different oxygen atoms approaching the miscoordinated silicon. After an oscillatory behavior, one of these oxygen atoms (labeled No. 5) got trapped, restoring the fourfold coordination.

In other typical diffusive events that we observed, an oxy-

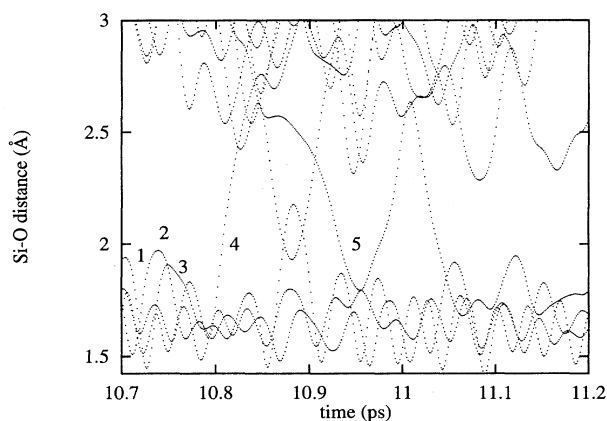


FIG. 2. Temporal dependence of the radial distance between a given silicon atom and its oxygen neighbors in liquid SiO_2 at 3500 K, illustrating a typical diffusive event. O atom No. 4 leaves the coordination sphere and is replaced by O atom No. 5 at the second attempt.

gen atom approached and bonded to a silicon atom making it fivefold coordinated. Within about 0.2 ps another Si-O bond broke, bringing the silicon atom back to fourfold coordination.

These observations suggest that diffusive events consist of temporary defects created by occasional neighbor exchanges which are subsequently restored in about 0.2 ps. This indicates that even when diffusive motion is taking place, the Si atoms are fourfold coordinated during most of the time. A typical diffusive event is characterized by a jumplike motion of an oxygen atom from the coordination sphere of a given Si atom to that of an adjacent Si atom. When this occurs, the missing oxygen is immediately replaced. Thus, a strong correlation is observed between jumplike events which give rise to defects and their subsequent restorations. This type of diffusive motion contrasts strongly with that of ordinary liquids which show a continuous diffusive motion and is consistent with the presence of a strong bond network even in the liquid phase. This kind of diffusive mechanism could also be inferred from classical simulations.⁵

IV. STRUCTURAL PROPERTIES

In Ref. 16, we found a very good agreement between calculated and experimental total neutron structure factors $S_N(q)$ for the amorphous. We note that this agreement was obtained without any other *a priori* knowledge than the volume of the simulation cell. Therefore, in contrast to simulations with classical potentials, the remarkable agreement with experiment does not stem from fitting procedures, and provides strong support for other physical quantities, which are not directly available from experiment, such as the partial pair correlation functions and the bond-angle distributions.

A. Partial pair correlation functions

The average partial pair correlation functions as found from our MD simulation of liquid and vitreous SiO_2 are given in Fig. 3. Except for a high-temperature broadening of

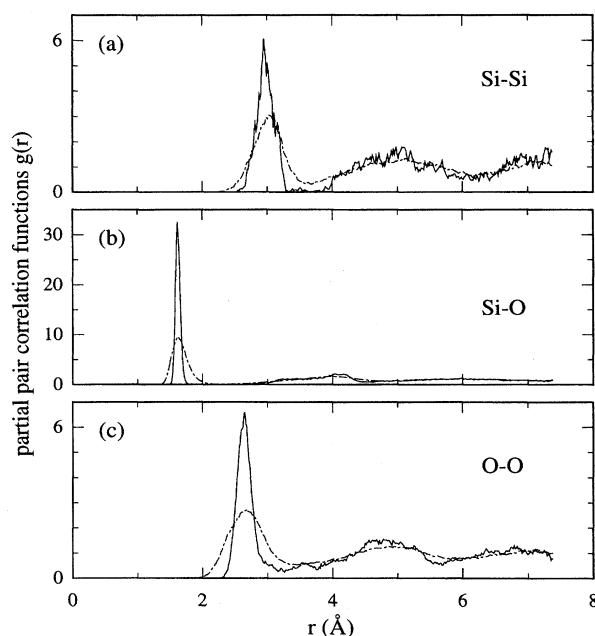


FIG. 3. Partial pair correlation functions in liquid SiO_2 (dash-dotted line) and vitreous SiO_2 (solid line).

the features, no particular difference can be noticed between the pair correlation functions in the liquid and in the glass. Overall, our pair correlation functions for both liquid and vitreous SiO_2 are similar to those found in recent classical MD calculations.⁸ A minor difference consists in the position of the first peak in the Si-Si pair correlation, which, in our simulation, is found to be slightly displaced towards smaller values (by about 3%).²⁴ This property is directly related to the Si-O-Si bond-angle distribution, which is the subject of the next subsection.

In the case of the glass, integration of the area in the first peak in the Si-O correlation function gives four, indicating perfect chemical order, i.e., all Si and O atoms are found to be fourfold and twofold coordinated, respectively. In the liquid, we find a broader distribution of Si-O distances because diffusion occurs by breaking bonds and generating defects. However, even in this case the persistence of a strong network was observed, with a small amount of miscoordinated atoms. These consisted of threefold and fivefold coordinated silicon and of onefold and threefold coordinated oxygen atoms. We have studied in Fig. 4 their relative occurrence as a function of the coordination radius. In Fig. 4(a), for a given coordination radius, we give the average percentage of Si atoms with three, four, and five nearest-neighbor oxygen atoms. In Fig. 4(b), we give the average number of onefold, twofold, and threefold coordinated oxygen atoms. Considering that a typical Si-O bond length is about 1.6 Å, one notices that most of the defects correspond to undercoordinated atoms, namely, trivalent silicon atoms and nonbridging oxygen atoms. Indeed, these defects often occur together and arise as a consequence of the breaking of a Si-O bond. The broken bond $\text{O}^- + \text{Si}^+$ can be considered as the intrinsic precursor of the paramagnetic defects observed in electron spin resonance.^{25,26}

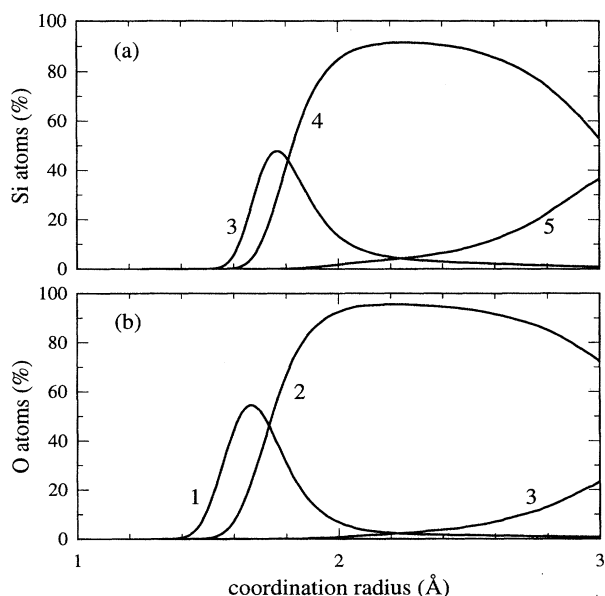


FIG. 4. Average coordination of (a) Si and (b) O atoms in liquid SiO₂ as a function of the radius of the coordination sphere. The coordination is defined as the number of first nearest neighbors in the coordination sphere.

B. Bond-angle distributions

1. O-Si-O bond-angle distribution

The distributions of the O-Si-O bond angles in the liquid and in the glass are shown in Fig. 5. The average angle of both distributions is close to 109°, indicating that Si centered tetrahedra are the structural units of both the liquid and the glass. The sharpness of the distribution in the case of the glass is remarkable and points out the presence of strong directional bonds.

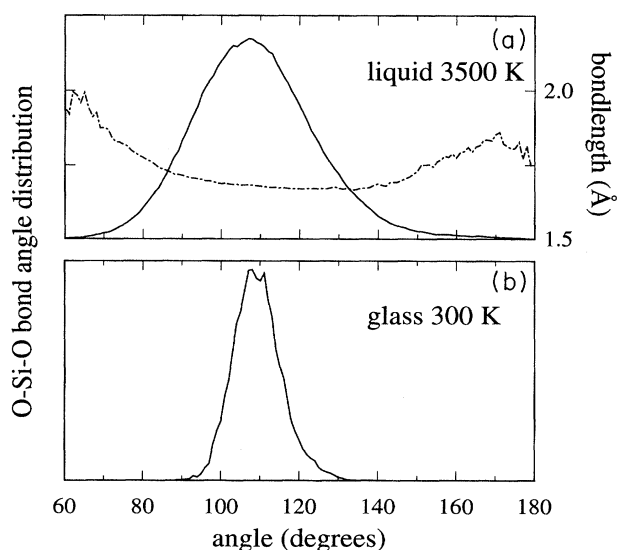


FIG. 5. O-Si-O bond-angle distributions in (a) liquid and (b) vitreous SiO₂. The dash-dotted line in (a) describes the average Si-O distance as a function of the O-Si-O bond angle in the liquid.

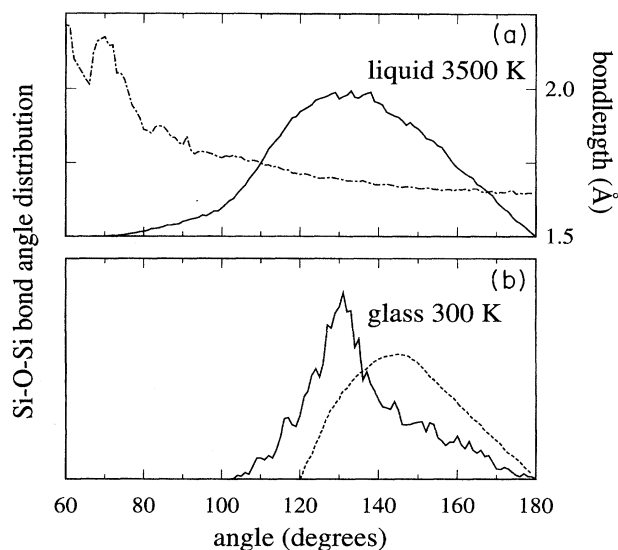


FIG. 6. Si-O-Si bond-angle distributions in (a) liquid and (b) vitreous SiO₂. The dash-dotted line in (a) describes the average Si-O distance as a function of the Si-O-Si bond angle in the liquid. The dashed line is taken from Ref. 27 and was extracted from x-ray diffraction spectra.

In order to investigate the correlation between bond lengths and bond angles in the liquid, we also report in Fig. 5 the average Si-O bond length in a O-Si-O group as a function of the bond angle. One can see that in the range of the most probable bond angles the average bond length is rather constant and that its value corresponds to the peak position of the Si-O pair correlation displayed in Fig. 3. Bond lengths which correspond to angles which occurred with low probability are larger than the typical bond length and contribute to the tail on the high-value side of the Si-O nearest-neighbor peak in Fig. 3.

2. Si-O-Si bond-angle distribution

Disorder in liquid and vitreous SiO₂ derives from the flexibility of the bridging angle between corner-sharing tetrahedral units, giving rise to a broad Si-O-Si bond-angle distribution. Therefore, the shape of this distribution is a direct characterization of the disorder in these systems. It is extremely difficult to extract the Si-O-Si bond angle distribution in vitreous SiO₂ directly from experiment. Such distributions can be obtained from, e.g., x-ray diffraction or NMR data, but rely on underlying theoretical models for the disorder. Also classical MD simulations have been unsuccessful in predicting this bond angle distribution, as can be deduced from the large variety of results obtained over the years with different potentials. In this context, a Si-O-Si bond-angle distribution derived from first principles is of particular interest.

In Fig. 6, we give the Si-O-Si bond-angle distributions for liquid and vitreous SiO₂ as obtained from our simulation. The average values of these distributions are 134° and 136° for the liquid and the glass, respectively, slightly smaller than typical values in crystalline forms of SiO₂.⁸

The distribution for the liquid is particularly broad and presents a tail which extends down to angles as small as

70°. In the glass, this tail on the small angles side has mostly disappeared and the distribution extends from about 110° to 180°. A bond-angle distribution extending below 120° would allow for edge-sharing tetrahedra. Indeed a few edge-sharing tetrahedra were found in the liquid at $T=3500$ K, but these configurations were absent in our vitreous sample. Again, in a similar way as in Fig. 5, we have studied the correlation between bond lengths and bond angles. In Fig. 6, one notices that the tail towards small bridging angles present in the case of the liquid is correlated to an increase in the average bond length. Thus, the bond-breaking mechanism necessary for diffusion in the liquid seems to be related to a twisting of bond angles.

It is interesting to note that the overall shape of the distribution in the liquid, namely, with a tail on the small angles side and skewed to large angles, is characteristic for a system with reduced directional effects, as can be deduced from simulations with two-body potentials.⁷ In the model of the glass, the shape of the distribution is rather different. It presents a rapid falloff around 120° and a tail towards higher angles.

In Fig. 6, we have also reported the distribution extracted from x-ray diffraction data by Mozzi and Warren.²⁷ Although the shape of this distribution, in particular the rapid falloff on the small angles side, resembles the one obtained from our simulation, its mean value is shifted towards larger values (144° vs 136°). Analysis of NMR data also gives larger mean values (140°–150°, Ref. 28). However, the extraction of a bond-angle distribution from either x-ray or NMR data is not free from theoretical assumptions, and carries therefore a considerable degree of uncertainty.

We remark that, among the properties considered in this work, it is the Si-O-Si bond-angle distribution which undergoes the most important change when our SiO₂ sample is quenched from the melt. Whereas the other structural properties in our vitreous sample merely exhibit reduced broadening effects due to the lower temperature, the Si-O-Si bond-angle distribution shows a qualitative transformation as discussed above. This change derives from a variation of the chemical bonding properties with temperature. Classical potentials have difficulties in describing these effects. Indeed, no qualitative change in the Si-O-Si bond-angle distribution has been observed in recent classical MD simulations.⁸

V. ELECTRONIC PROPERTIES

In this section we present a comparative study of the calculated electronic density of states (DOS) in liquid, vitreous, and crystalline SiO₂ at different temperatures. In Fig. 7, we give the DOS of the liquid at 3500 and 3000 K, of the glass at 300 K, and of α -quartz at 300 and 0 K.

The common features of the DOS in Fig. 7 result from the similar short-range order in the various forms of SiO₂. The states can be classified in the same way: the states at about -20 eV are oxygen 2s states, the states from -10 to -4 eV are bonding states between Si sp^3 hybrids and mainly O 2p orbitals, the highest occupied states above -4 eV are O 2p nonbonding orbitals, while the lowest conduction band states have antibonding character.^{11,30}

The DOS of α -quartz in Fig. 7(e) agrees well with that of other calculations; in particular, we obtain for the band gap a

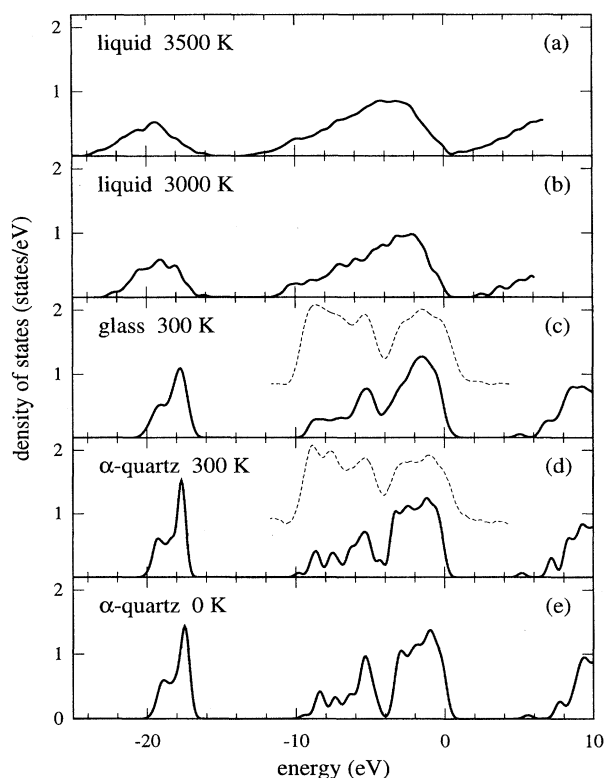


FIG. 7. Electronic density of states of SiO₂: (a) liquid at 3500 K, (b) liquid at 3000 K, (c) glass at 300 K, (d) α -quartz at 300 K, and (e) α -quartz at 0 K. Dashed curves are taken from XPS experiments. (Ref. 30). In the theoretical curves the Fermi energy is at 0 eV. The presented data are the result of a convolution with a Gaussian of width $\sigma=0.25$ eV.

value of 5.6 eV to be compared with a value of 5.8 eV of Ref. 11. As usual within LDA calculations, the theoretical band gap substantially underestimates the experimental band gap, which is about 9 eV.²⁹

In Figs. 7(c) and (d), we compare the calculated DOS to experimental photoemission spectra for the glass and α -quartz, respectively.³⁰ Considering the presence of a smoothly varying background in the experimental spectra and the absence of state-dependent transition probabilities in the DOS, the overall agreement can be considered very good.

Our study shows that the electronic band gap in SiO₂ systems is extremely sensitive to thermal vibrations and to structural disorder. The band gap in α -quartz decreased by 0.5 eV, when the temperature was raised from 0 to 300 K [see Figs. 7(e) and (d)]. This is in good qualitative agreement with experiment, where a band gap reduction of 0.4 eV was found, when the temperature was raised from 173 to 373 K.³¹ Notice that this change of the gap results from mere thermal vibrations of the atoms. When structural disorder is also present as in the glass at 300 K [Fig. 7 (c)], the gap is lowered by another 0.3 eV. This trend also agrees qualitatively with experiment, where the fundamental absorption edge of vitreous SiO₂ is found to be lower than that of α -quartz by approximately 0.5 eV.³¹

The dependence of the band gap on structural disorder

was also seen when liquid SiO₂ was cooled from 3500 to 3000 K [Figs. 7(a) and (b)]. At 3500 K a large broadening of the bands led to a complete closing of the gap [Fig. 7(a)].³² As a consequence of the cooling to 3000 K, the band gap increased by 2 eV. This effect can be attributed to the broader distributions of bond lengths and angles at higher temperature. On one hand, the splitting between O *p*-Si *sp*³ bonding and antibonding states decreased, thus introducing unoccupied electronic states in the gap. On the other hand, the variations in the Si-O-Si angle broadened the bandwidth of the oxygen *p* states, filling the band gap with occupied states.

VI. CONCLUSIONS

We have presented additional information on *ab initio* molecular-dynamics simulations of liquid and vitreous SiO₂, which complements the description given in a recent paper.¹⁶ First, we studied the diffusive motion of an equilibrated liquid at 3500 K. In particular, we studied bond length and bond-angle distributions, miscoordinated atoms, and aspects related to the diffusion mechanism.

Then, we turned to the model for the glass, which can be characterized as a perfectly chemically ordered bond net-

work. We obtained partial pair correlation functions which are yet unknown from experiment and presented the shape of the bond-angle distribution functions.

We calculated electronic DOS of liquid and vitreous SiO₂ and compared them to that of α -quartz. By studying the temperature dependence of the DOS, we found that the enhancement of disorder produces a progressive reduction of the gap.

In conclusion, we have generated a model of vitreous SiO₂, which presents good agreement with experiment for both structural and electronic properties. This work is the first step towards accurate quantitative studies of defects in vitreous SiO₂, in which the interplay between structural and electronic properties is of fundamental importance.

ACKNOWLEDGMENTS

We acknowledge support from the Swiss National Science Foundation under Grant No. 20-39528.93. One of us (J.S.) has benefited from a grant of the Swiss "Commission fédérale des bourses pour étudiants étrangers." Calculations have been performed on the NEC-SX3 of the Swiss Center for Scientific Computing (CSCS) in Manno.

-
- ¹ *The Physics and Technology of Amorphous SiO₂*, edited by R. A. B. Devine (Plenum Press, New York, 1988).
- ² S.R. Elliot, *The Physics of Amorphous Materials*, 2nd ed. (Longman, London, 1990).
- ³ *The Physics of SiO₂ and its Interfaces*, edited by S. T. Pantelides (Pergamon Press, New York, 1978).
- ⁴ R. Brückner, *J. Non-Cryst. Solids* **5**, 123 (1970).
- ⁵ L. V. Woodcock, C. A. Angell, and P. Cheeseman, *J. Chem. Phys.* **65**, 1565 (1976).
- ⁶ T. F. Soules, *J. Chem. Phys.* **71**, 4570 (1979); S. K. Mitra, M. Amini, D. Fincham, and R. W. Hockney, *Philos. Mag. B* **43**, 365 (1981); B. P. Feuston and S. H. Garofalini, *J. Chem. Phys.* **65**, 1565 (1988); B. Vessal, M. Amini, D. Fincham, and C.R.A. Catlow, *Philos. Mag. B* **60**, 753 (1989); J. R. Rustad, D. A. Yuen, and F. J. Spera, *Phys. Rev. A* **42**, 2081 (1990).
- ⁷ J. D. Kubicki and A. C. Lasaga, *Am. Mineral.* **73**, 941 (1988).
- ⁸ P. Vashishta, R. K. Kalia, J. P. Rino, and I. Ebbsjö, *Phys. Rev. B* **41**, 12 197 (1990).
- ⁹ F. Liebau, in *The Physics and Technology of Amorphous SiO₂* (Ref. 1).
- ¹⁰ D. C. Allan and M. P. Teter, *Phys. Rev. Lett.* **59**, 1136 (1987); D. C. Allan and M. P. Teter, *J. Am. Ceram. Soc.* **73**, 3247 (1990); C. Lee and X. Gonze, *Phys. Rev. Lett.* **72**, 1686 (1994); X. Gonze, J. C. Charlier, D. C. Allan, and M. P. Teter, *Phys. Rev. B* **50**, 13 035 (1994); F. Liu, S. H. Garofalini, R. D. King-Smith, and D. Vanderbilt, *Phys. Rev. Lett.* **70**, 2750 (1993).
- ¹¹ N. Binggeli, N. Troullier, J. L. Martins, and J. R. Chelikowsky, *Phys. Rev. B* **44**, 4771 (1991).
- ¹² X. Gonze, D. C. Allan, and M. P. Teter, *Phys. Rev. Lett.* **68**, 3603 (1992).
- ¹³ R. Car and M. Parrinello, *Phys. Rev. Lett.* **55**, 2471 (1985).
- ¹⁴ For a review, see G. Galli and A. Pasquarello, in *Computer Simulation in Chemical Physics*, edited by M. P. Allen and D. J. Tildesley (Kluwer, Dordrecht, 1993), p. 261.
- ¹⁵ D. Vanderbilt, *Phys. Rev. B* **41**, 7892 (1990).
- ¹⁶ J. Sarnthein, A. Pasquarello, and R. Car, *Phys. Rev. Lett.* **74**, 4682 (1995).
- ¹⁷ I. T. Penfold and P. S. Salmon, *Phys. Rev. Lett.* **67**, 97 (1991).
- ¹⁸ S. R. Elliot, *Phys. Rev. Lett.* **67**, 711 (1991).
- ¹⁹ P. S. Salmon, *Proc. R. Soc. London A* **437**, 591 (1992).
- ²⁰ M. Wilson and P. A. Madden, *Phys. Rev. Lett.* **72**, 3033 (1994).
- ²¹ A. B. Bhatia and D. E. Thornton, *Phys. Rev. B* **2**, 3004 (1970).
- ²² A. Pasquarello, K. Laasonen, R. Car, C. Lee, and D. Vanderbilt, *Phys. Rev. Lett.* **69**, 1982 (1992); K. Laasonen, A. Pasquarello, R. Car, C. Lee, and D. Vanderbilt, *Phys. Rev. B* **47**, 10 142 (1993).
- ²³ The error bars have been determined by considering the fluctuations of the mean square displacement in our MD simulation. Due to the limited statistics, our error estimates should only be taken as indicative.
- ²⁴ A table containing information regarding the first peaks has been provided in Ref. 16.
- ²⁵ G. N. Greaves, *J. Non-Cryst. Solids* **32**, 295 (1979).
- ²⁶ E. P. O'Reilly and J. Robertson, *Phys. Rev. B* **27**, 3780 (1983).
- ²⁷ R. L. Mozzi and B. E. Warren, *J. Appl. Cryst.* **2**, 164 (1969).
- ²⁸ R. Dupree and R. F. Pettifer, *Nature* **308**, 523 (1984).
- ²⁹ F. J. Himpsel, *Surf. Sci.* **168**, 764 (1986); F. J. Grunthaner and P. J. Grunthaner, *Mater. Sci. Rep.* **1**, 65 (1986).
- ³⁰ R. B. Laughlin, J. D. Joannopoulos, and D. J. Chadi, *Phys. Rev. B* **20**, 5228 (1979); B. Fischer, R. A. Pollak, T. H. DiStefano, and W. D. Grobman, *ibid.* **15**, 3193 (1977).
- ³¹ A. Appleton, T. Chiranjivi, and M. Jafaripour, in *The Physics of SiO₂ and its Interfaces* (Ref. 3).
- ³² The fact that the gap is closed at 3500 K might be an artifact of LDA. However, we expect the trends as a function of temperature to be reliable.